Carbohydrate Research 413 (2015) 70–74

Contents lists available at ScienceDirect

Carbohydrate Research

journal homepage: www.elsevier.com/locate/carres

Probing the roles of conserved residues in uridyltransferase domain of *Escherichia coli* K12 GlmU by site-directed mutagenesis

Shuaishuai Wang [a, b, †], Xuan Fu [a, †], Yunpeng Liu [b, c], Xian-wei Liu [a], Lin Wang [d], Junqiang Fang [a, *], Peng George Wang [a, c]

[a] National Glycoengineering Research Center, Shandong University, Jinan, Shandong 250100, People's Republic of China
[b] The State Key Laboratory of Microbial Technology and School of Life Sciences, Shandong University, Jinan, Shandong 250100, People's Republic of China
[c] Department of Chemistry, Georgia State University, P.O. Box 4098, Atlanta, GA 30302-4098, USA
[d] Department of Food Science and Engineering, Nanshan University, Yantai, Shandong 265713, People's Republic of China

ARTICLE INFO

Article history:
Received 13 April 2015
Received in revised form
18 May 2015
Accepted 21 May 2015
Available online 2 June 2015

Keywords:
Uridyltransferase
UDP-GlcNAc
Substrate specificity
Site-directed mutagenesis

ABSTRACT

N-Acetylglucosamine-1-phosphate uridyltransferase (GlmU) is a bifunctional enzyme that catalyzes both acetyltransfer and uridyltransfer reactions in the prokaryotic UDP-GlcNAc biosynthesis pathway. Our previous study demonstrated that the uridyltransferase domain of GlmU (tGlmU) exhibited a flexible substrate specificity, which could be further applied in unnatural sugar nucleotides preparation. However, the structural basis of tolerating variant substrates is still not clear. Herein, we further investigated the roles of several highly conserved amino acid residues involved in substrate binding and recognition by structure- and sequence-guided site-directed mutagenesis. Out of total 16 mutants designed, tGlmU Q76E mutant which had a novel catalytic activity to convert CTP and GlcNAc-1P into unnatural sugar nucleotide CDP-GlcNAc was identified. Furthermore, tGlmU Y103F and N169R mutants were also investigated to have enhanced uridyltransferase activities compared with wide-type tGlmU.

1. Introduction

Uridine 5′-diphosphate *N*-acetylglucosamine (UDP-GlcNAc), an important cytoplasmic amino sugar nucleotide and the activated form of GlcNAc, is the key precursor in enzymatic glycosylation by Leloir-type glycosyltransferases to create incredible diversity of glycoconjugates, including cell wall peptidoglycans,[1] lipopolysaccharides,[2] glycosaminoglycans,[3] enterobacterial common antigens,[4] chitin[5] and protein N-and O-linked glycans.[6,7] Although UDP-GlcNAc has been widely used for many years, much still remains unknown about its functional mechanisms and synthetic pathway. Chemical synthesis of UDP-GlcNAc and its derivatives have been developed, but the low yield and fastidious process hinder its application.[8,9] In contrast, enzymatic synthesis, which mimics the biosynthetic pathway is considered more attractive with the advantages of high region-/stereo-specificity and low cost.

N-Acetylglucosamine-1-phosphate uridyltransferase (GlmU) is a key bifunctional enzyme with both acetyltransferase (EC 2.3.1.157) and uridyltransferase (EC 2.7.7.23) activities, which catalyzes the formation of UDP-GlcNAc from glucosamine-1-P, acetyl-CoA and UTP in prokaryotic UDP-GlcNAc de novo biosynthetic pathway.[10] The bacterial GlmU has been well studied from *Escherichia coli*, *Haemophilus influenza*, and *Streptococcus pneumonia*.[10–12] The N-terminal uridyltransferase domain of GlmU belongs to the nucleoside triphosphate transferase superfamily and shares signature sequence motif of L-X_2-G-X-G-T-X-M-X_4-P-K.[13]

Till now, a series of GlmU crystal structures have been solved.[11,12] The reported crystal structure of GlmU (1HV9, PDB) demonstrates that the overall structure of the uridyltransferase domain is that of a seven-stranded mixed α-helix surrounded by six β-sheets and a two-stranded α-helix sitting atop the larger mixed sheet.[14,15] This domain can be divided into two substrate-binding regions. The region that binds to the uridine of UTP, consists of Ala12-Gly14, Ala18, Lys25, Gln76-Thr82, and Asp105 structural segments and forms a solvent-exposed pocket. The region that binds to GlcNAc moiety, includes strands β5-β7 and interacts primarily with the GlcNAc moiety of GlcNAc-1-P.

We previously cloned the uridyltransferase domain of *E. coli* K12 GlmU, tGlmU, which had a smaller molecular weight and higher soluble expression level, remained comparable catalytic activity

* Corresponding author. Tel.: +86 531 88366078; fax: +86 531 88363002.
E-mail address: fangjunqiang@sdu.edu.cn (J. Fang).
† Same contribution to this paper.

http://dx.doi.org/10.1016/j.carres.2015.05.007
0008-6215/

with the full-length GlmU.[16] This truncated tGlmU could also recognize several nucleoside triphosphates (NTPs) to form the corresponding sugar nucleotides in lower efficiencies. Although the GlmU crystal structure has been available, the roles of highly conserved residues in substrate-binding regions are still unclear, leading to some uncertainty concerning residues involved in substrate binding and enzyme reaction. In order to probe the roles of these highly conserved residues, structure- and sequence-guided mutagenesis studies were carried out to broad substrate specificity and to improve catalytic efficiency for the formation of sugar nucleotides. Among mutants obtained by substituting the highly conserved residues in substrate-binding regions, tGlmU Q76E mutant with altered catalytic activity toward the formation of unnatural sugar nucleotide CDP-GlcNAc was identified. Two tGlmU mutants, Y103F and N169R with significantly enhanced uridyltransferase activities were also identified. The structural and biochemical characterization of the uridyltransferase active sites and catalytic mechanism described herein deepened our understanding about mechanisms of GlmU reactions.

2. Results and discussion

2.1. Crystal structure-based design of tGlmU mutants

Based on the sequence alignment of homologous proteins and crystal structure data, several highly conserved amino acid residues, which involved in the interactions with UDP-GlcNAc through hydrogen bonds were identified (Fig. 1). In order to probe the roles of these highly conserved residues in catalytic activity, we substituted residue Gln76 in the uridine-binding region and Thr82, Glu154, Asn169 in the GlcNAc-binding region, respectively. Two other residues, Tyr103 and Asp105, which located nearby the uridyltransferase active pocket, were also investigated.

All the mutants designed were transformed into *E. coli* BL21(DE3) strains and subsequently overexpressed under standard conditions as previously described for tGlmU.[16] The soluble protein expression levels of wide-type tGlmU or mutants were approximately 40 mg/L.

2.2. Roles of highly conserved residue Gln76

GlmU structure data demonstrates that UTP substrate is involved in extensive hydrogen bond networks formed between its functional groups and protein atoms of the active site cavity, either directly or water-mediated. The uracil base is reinforced by two hydrogen bonds between its exocyclic N3, O4 ring atoms and Gln76 side chain Oε1, Nε2, respectively. This key residue was proposed to play important role in overall catalytic activity of the enzyme. In order to determine the necessity of this highly conserved residue involved in substrate recognition and catalytic activity, mutants (Q76E, Q76A, Q76P) were constructed and analyzed (Fig. 2).

To our delight, a unique catalytic activity of tGlmU Q76E mutant was identified. We observed that cytidine 5′-triphosphate (CTP), which had an amide group instead of a carbonyl group on the base, could be accepted and converted to unnatural sugar nucleotide CDP-GlcNAc with a yield of 53.1%. However, the uridyltransferase activity of Q76E mutant decreased dramatically, as about half of the activity of the wild-type tGlmU. Hydrogen bonds, which formed between hydrogen atoms and electronegative hydrogen bond acceptors, usually are relatively weak interactions but nonetheless are crucial for enzymatic catalytic reactions. Apparently, the substitution of Gln76 to Glu residue disrupted the initial hydrogen-bonded interaction between residue Gln76 and exocyclic oxygen O4 of the uracil base, leading to poor conversion efficiency to form UDP-GlcNAc. Interestingly, the exocyclic amide group of unnatural substrate CTP, which acted as the hydrogen bond acceptor, could form a nascent hydrogen bond with side chain of the substituted Glu residue, thus facilitating CTP to enter to the uridyltransferase pocket and endowing Q76E mutant a novel activity to form unnatural sugar nucleotide CDP-GlcNAc. We further measured that the optimal pH slightly changed from 8.0 to 7.5 followed by the substitution of Gln76 residue to Glu (Fig. 3).

Beside the Q76E mutant, we designed other two mutants Q76A and Q76P to fully demonstrate the role of this key residue. Q76A mutant showed that the uridyltransferase activity decreased dramatically (40% activity of the wide-type tGlmU), presumably resulting from the weakened hydrogen bond interaction caused by mutagenesis. In contrast, the substitution of Gln76 with Pro residue resulted in a slightly enhancement to UTP recognition and catalytic activity (nearly 1.1 fold compared with the wide-type tGlmU).

2.3. Roles of highly conserved residues in GlcNAc-binding region

GlmU crystal structure indicates that the GlcNAc moiety is involved in extensive hydrogen bond network formed between its hydroxyl groups and protein atoms of the active site cavity, either directly or water-mediated. The GlcNAc-binding region consisting of Thr82, Tyr103, Thr137-Gln140, Glu154, and Asn169-Glu171 structural segments arranges to recognize the GlcNAc in GlcNAc-1-P and structural rearrangements required to complete the uridyltransferase reaction. The *N*-acetyl moiety is recognized by two hydrogen bonds between its N2′ and Glu154, as well as between its O7′ and Thr82, respectively. In order to probe the necessity of these highly conserved residues involved in substrate recognition and

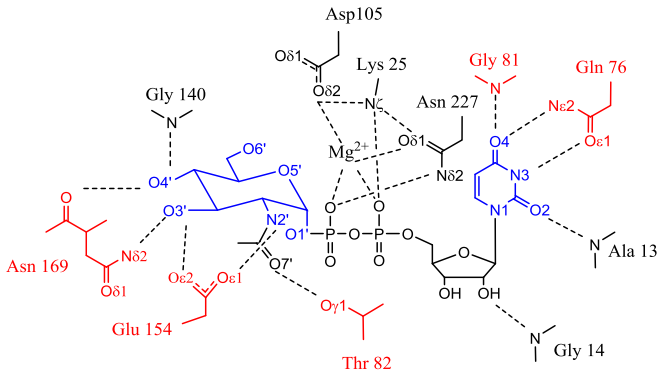

Fig. 1. Schematic drawing of hydrogen bonds between UDP-GlcNAc and residues in the uridyltransferase active site of *E. coli* K12 GlmU.

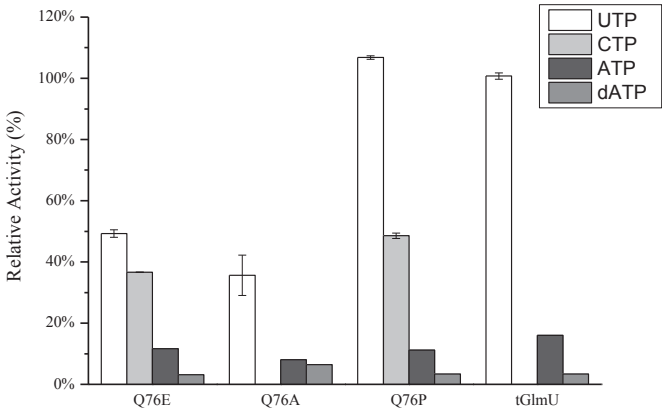

Fig. 2. Comparative uridyltransferase activity of tGlmU Gln76 mutants. The activity for wide-type tGlmU was set to 100%.

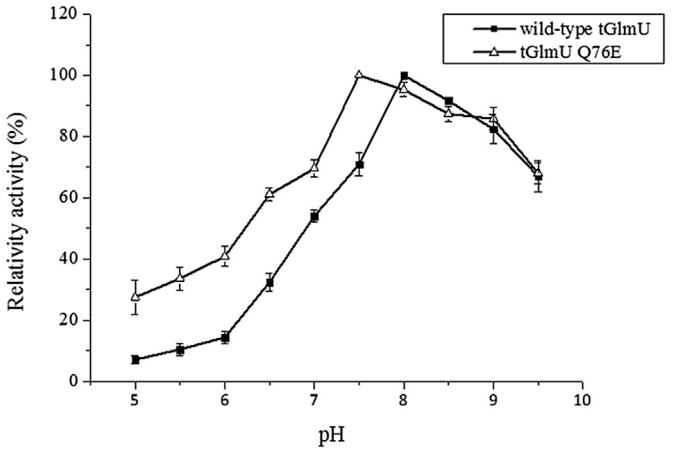

Fig. 3. Effects of pH on wild-type tGlmU and tGlmU Q76E mutant activities.

catalytic activity, residues Thr82, Glu154, and Asn169 were investigated by site-directed mutagenesis (Fig. 4).

Residue Thr82 locates on the α-helix nearby the uridyltransferase pocket and is proposed to be an important residue for recognition of the *N*-acetyl arm of GlcNAc. Therefore, the polar uncharged residue Thr82 was constructed to Ser (T82S), Gln (T82Q), and Gly (T82G). Activity assays using GlcNAc-1-P as sugar-1-P donor showed that T82S, T82Q and T82G mutants impaired the uridyltransferase activities (21–35% activity of the wide-type tGlmU). Moreover, none of these three mutants could tolerance C2 modified sugar-1-P derivatives (Glc-1-P, Glcz-1-P) as substrate to form the corresponding sugar nucleotides. These results indicated that sugar-1-P stabilizing effect by Thr82 hydrogen-bonded interaction was more significant when GlcNAc-1-P, instead of Glc-1-P or Glcz-1-P, was used as the substrate. Substitution to larger residues Gln, Ser, or to the simple residue Gly did not provide assistance in stabilizing the interaction between sugar-1-P and the enzyme.

The functionally important residue Glu154 is highly conserved in most related bacterial sugar nucleotide uridyltransferases. In tGlmU, Glu154 locates on the β-turn secondary structure and forms two hydrogen bonds with the *N*-acetyl arm and C3 hydroxyl group of GlcNAc moiety, respectively. Altering residue Glu154 with Asp (E154D) or with a hydrophobic residue Leu (E154L) showed that the uridyltransferase activities decreased drastically (nearly 20% activity of the wide-type tGlmU). Substitution of Glu154 with a positive residue Lys (E154K) thoroughly impaired its activity, presumably resulting from the slightly secondary conformation changes caused by mutation. These results indicated that both the hydrogen bonds formed by residue Glu154 and its negative charged side chain were necessary to provide benefit in accommodating GlcNAc-1-P as substrate for uridyltransferase reaction.

Residue Asn169, which locates on the β-sheet secondary structure and forms two hydrogen bonds with GlcNAc motif, acts as a structural switch to drive the uridyltransferase active site into the closed conformation upon binding of UDP-GlcNAc. Substitution of Asn169 to a simply hydrophobic Ala residue (N169A) decreased the uridyltransferase activity (55% activity of the wide-type tGlmU), presumably resulting from the unstable substrate binding caused by the weakened hydrogen-bonded interactions. Altering Asn169 to Asp (N169D) or Gln (N169Q) did not affect the catalytic activities. Remarkably, N169R mutant, which was substituted by a positive charged Arg residue, showed an enhanced uridyltransferase activity (nearly 1.4 fold of the wide-type tGlmU). The secondary structure predication indicated that the N169R mutant caused a slightly secondary structure changes, thus facilitating GlcNAc-1-P to enter the active pocket through the additional interaction with N-acetyl arm of GlcNAc moiety (Fig. 5).

2.4. Roles of highly conserved residues near the uridyltransferase active pocket

Tyr103-Asp105 segment, which locates at the floor of the uridyltransferase active pocket, also involves in interactions with UTP

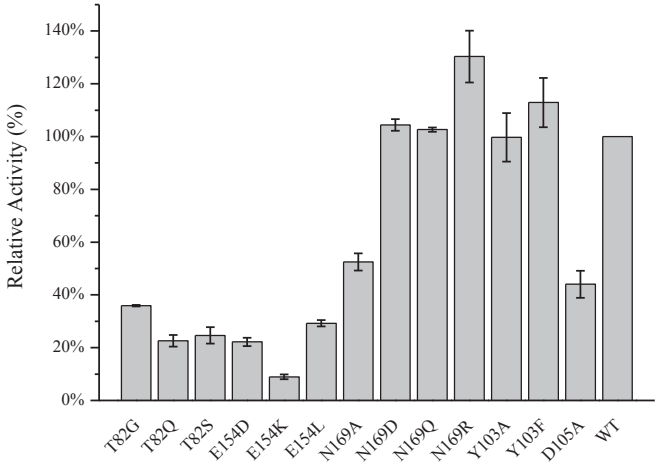

Fig. 4. Comparative uridyltransferase activity of tGlmU mutants constructed in GlcNAc-binding region. The activity for wide-type tGlmU was set to 100%.

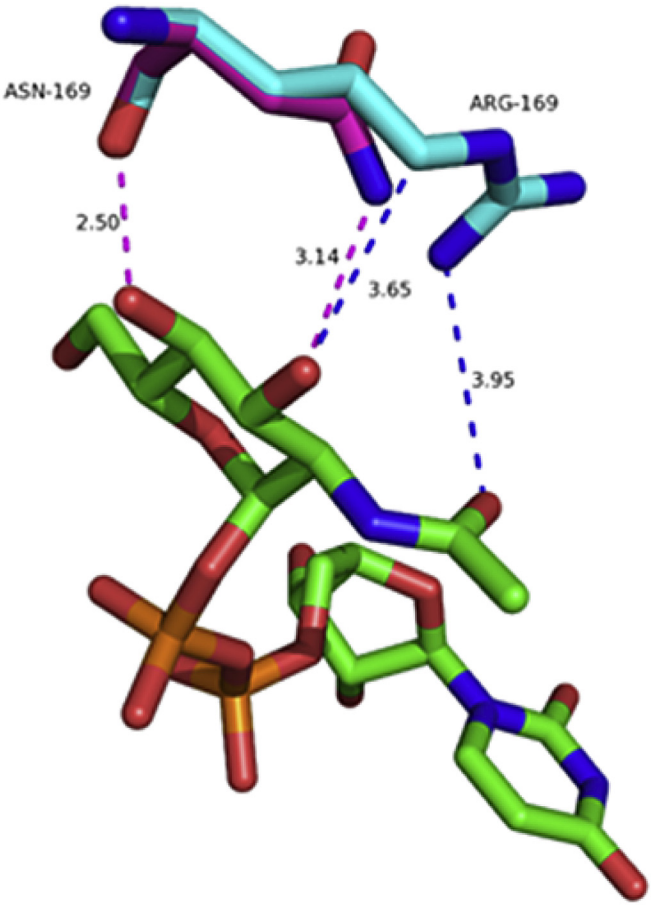

Fig. 5. Predication result of secondary structure changes caused by tGlmU N169R mutant.

and GlcNAc-1-P substrates. Previous studies indicated that this segment had significantly conformation changing during the enzyme reaction. In order to demonstrate the role of this segment, three mutants were constructed. Activity assay results indicated that two mutants occurred on Tyr103 residue (Y103A and Y103F) exhibited enhanced catalytic activities to form UDP-GlcNAc, especially Y103F, which had a 1.2 fold activity of the wide-type tGlmU. Based on structure data, we presumed that it was the hydrophobic characteristic of Tyr103 residue that affected the enzymatic reaction. Substitution to other hydrophobic residues might contribute to substrate-enzyme interactions, thus facilitating GlcNAc-1-P and UTP to enter the uridyltransferase pocket. In contrast, the tGlmU D105A mutant, which affected the adjacent hydrophobic interactions, impaired its activity (two folds lower than the wide-type tGlmU).

2.5. The secondary structure changes in tGlmU mutants

In order to fully understand the functional roles of the tGlmU mutants, we predicated the secondary structures by SWISS-MODEL Workspace to calculate conformation changes (Table 1). The predication results demonstrated that all the mutants did not affect the secondary structures where the mutated residues located. However, substitution of the corresponding residues had effect on the secondary structures formed by the amino acids adjacent and far way from these mutated residues.

2.6. Enzymatic synthesis of unnatural CDP-GlcNAc by coupling of Q76E mutant and NahK

In order to demonstrate the application of tGlmU Q76E mutant for unnatural sugar nucleotide preparation, we performed a one-pot de novo CDP-GlcNAc synthetic reaction. To facilitate the biosynthesis reaction, the *N*-acetylhexosamine 1-kinase from *Bifidobacterium longum* (NahK), which could convert ATP and GlcNAc into GlcNAc-1-P, was combined with tGlmU Q76E mutant.[17] The purified CDP-GlcNAc was identified by ESI-MS and compared with the CDP-GlcNAc produced by CjGlmU in our previous work.[18]

3. Conclusion

In summary, GlmU is a key cytoplasmic enzyme involved in prokaryotic UDP-GlcNAc biosynthetic pathway and an attractive target for antibiotic drug discovery. Based on our previous study, we investigated the functional roles of several highly conserved residues in the uridyltransferase domain of *E. coli* GlmU. Among mutants constructed in our experiment, tGlmU Q76E mutant exhibited a novel catalytic activity to convert CTP and GlcNAc-1-P into CDP-GlcNAc. Two other mutants, Y103F and N169R, showed enhanced activities toward the formation of UDP-GlcNAc. This work deepens our understanding of the reaction mechanisms of GlmU. The results further illuminate the relationship of highly conserved residues and enzyme reaction. Most importantly, site-directed mutagenesis provides a prototypic template for a structure-function analysis of the catalytic domains of uridyltransferases, which will benefit us to assess the roles of sequence-conserved residues in the catalytic mechanism.

4. Experimental section

4.1. Material

E. coli BL21(DE3) strain hosting the *E. coli* K12 *tGlmU* gene was constructed in our Lab previously.[16] Fast Multi-site-mutagenesis kit was from Transgen Biotechnology Company. Sugar-1-Ps and NTPs were from Sigma.

4.2. Site-directed mutagenesis

Site-directed mutagenesis was carried out using the Fast Multi-site-mutagenesis kit according to the protocol from the manufacturer. The primers used were shown in Table 2.

4.3. Protein expression of wide-type tGlmU and mutants

All mutants constructed were further confirmed by sequencing and subsequently transformed into *E. coli* BL21(DE3) strain for protein expression. The *E. coli* cells were cultured in Luria–Bertani medium supplemented with 100 μg/mL ampicillin. When OD_{600} reached 0.6–0.8, isopropyl-1-thio-β-D-galactopyranoside was added to a final concentration of 1 mM. The induced culture was further incubated at 28 °C for 3 h with shaking at 200 rpm. Cells were harvested by centrifugation at 12,000 rpm for 5 min. Protein purification was performed utilizing Ni-NTA resin (Amersham) according to the manufacturer's instructions at 4 °C. The purified

Table 1
The secondary structure changes caused by tGlmU mutants

Mutant	Predicted amino acid residues related to changes of secondary structure[a]
Q76A	T29(E→H), L30(E→H), L71(E→C), F93(C→H)
Q76E	T29(E→H), L30(E→C), L71(E→C), Y103(E→C), E145(C→E)
Q76P	K25(H→C), E145(C→E)
T82Q	K25(H→C), T29(E→H), L30(E→H), L71(E→C), E145(C→E)
T82G	T29(E→H), L30(E→H), L71(E→C), T82(C→H), Y103(E→C), E145(C→E), Q164(C→H)
T82S	T29(E→H), L30(E→H), L71(E→C), T82(C→H), E195(C→E)
Y103A	T29(E→H), L30(E→H), F93(C→H), Y139(C→E), G140(C→E), E145(C→E)
Y103F	K25(H→C), T29(E→H), L30(E→H), F93(C→H), Y139(C→E), G140(C→E)
D105A	T29(E→H), L30(E→H), L71(E→C)
E154D	L71(E→C), L108(C→E), I109(C→E), R163(H→C)
E154L	T29(E→H), L30(E→H), L71(E→C), F93(C→H)
E154K	T29(E→H), L30(E→H), L71(E→C), E145(C→E)
N169A	L71(E→C), F93(C→H)
N169D	L71(E→C), L108(C→E), I109(C→E)
N169R	L71(E→C), F93(C→H), R163(H→C)
N169Q	K25(H→C), L71(E→C), E145(C→E)

C represents coil structure.
E represents extened→beta.
H represents helix.
[a] The secondary structure changes were predicted by SWISS-MODEL Workspace.

Table 2
Primers used for site-directed mutagenesis

1	Q76E forward	5′aactgggtgcttgaggcagagcagctgggtacgggtcatgc3′
	Q76E revise	5′agctgctctgcctcaagcacccagttaaggttgtcgtgtttg3′
2	Q76A forward	5′accttaactgggtgcttgcggcagagcagctg3′
	Q76A revise	5′ cgcaagcacccagttaaggttgtcgtctttc3′
3	Q76P forward	5′accttaactgggtgcttccggcagagcagctg3′
	Q76P revise	5′cggaagcacccagttaaggttgtcgtctttc3′
4	T82G forward	5′caggcagagcagctgggtgggggtcatgcaatgc3′
	T82G revise	5′ccacccagctgctctgcctgaagcacccagttaagg3′
5	T82Q forward	5′caggcagagcagctgggtcagggtcatgcaatgc3′
	T82Q revise	5′tgacccagctgctctgcctgaagcacccagttaagg3′
6	T82S forward	5′caggcagagcagctgggtagcggtcatgcaatgc3′
	T82S revise	5′gctacccagctgctctgcctgaagcacccagttaagg3′
7	Y103A forward	5′atgaagacattttaatgctcgccggcgacgtgcc3′
	Y103A revise	5′ggcgagcattaaaatgtcttcatcatcggcaa3′
8	Y103F forward	5′atgaagacattttaatgctcttcggcgacgtgcc3′
	Y103F revise	5′gaagagcattaaaatgtcttcatcatcggcaa3′
9	D105A forward	5′taatgctctacggcgccgtgccgctgatctctg3′
	D105A revise	5′ggcgccgtagagcattaaaatgtcttcatcat3′
10	E154D forward	5′gcaaagttaccggcattgttgaccacaaagatgc3′
	E154D revise	5′gtcaacaatgccggtaactttgccgttttcacggg3′
11	E154L forward	5′gcaaagttaccggcattgttttgcacaaagatgc3′
	E154L revise	5′aaaacaatgccggtaactttgccgttttcacggg3′
12	E154K forward	5′gcaaagttaccggcattgttcagcacaaagatgc 3′
	E154K revise	5′gaacaatgccggtaactttgccgttttcacggg 3′
13	N169R forward	5′gtcagattcaggagatccgcaccggcattctg3′
	N169R revise	5′cggatctcctgaatctgacgctgctcgtcgg3′
14	N169D forward	5′gtcagattcaggagatcgacaccggcattctg3′
	N169D revise	5′cgatctcctgaatctgacgctgctcgtcgg3′
15	N169Q forward	5′gtcagattcaggagatccagaccggcattctg3′
	N169Q revise	5′ctggatctcctgaatctgacgctgctcgtcgg3′
16	N169A forward	5′gtcagattcaggagatcgccaccggcattctg3′
	N169A revise	5′ggcgatctcctgaatctgacgctgctcgt3′

fraction was dialyzed with a 10K centrifugal filter to remove imidazole and buffer components. Protein concentration was quantified using Bradford protein assay kit according to the protocol from the manufacturer. The wide-type tGlmU was also expressed, purified, and quantified as the positive control. All the proteins were stored at −20 °C with 20% glycerol existed.

4.4. Activity assays for mutant enzymes

Enzymatic reactions were carried out under standard conditions in duplicates in a total 100 μL solution containing 100 mM Tris−HCl (pH 7.5), 100 mM NaCl, 5 mM sugar-1-P, 5 mM NTPs, 5 mM $MgCl_2$, and 1 U/mL pyrophosphatase. The reactions were performed at 37 °C for 60 min and quenched by boiling at 100 °C for 5 min followed by centrifugation at 13,000 rpm for 15 min. The consumption of NTP and the formation of sugar nucleotide during reactions were analyzed by capillary electrophoresis (CE).

The products were characterized by a P/ACE MDQ Capillary Electrophoresis System. Electrophoresis was run in 75 μm×50 cm (40 cm to detector) bare fused silica capillary, under 25 kV with UV detection at 254 nm.

4.5. tGlmU Q76E mutant catalyzed the formation of CDP-GlcNAc

The one-pot two-enzyme synthetic reaction was carried out coupling of tGlmU Q76E mutant and NahK. The reaction system contained 5 mM GlcNAc, 5 mM CTP and 5 mM ATP in a final volume of 10 mL and incubated at 37 °C for 48 h. Yeast inorganic pyrophosphatase, which could drive the reaction forward by consuming the byproduct pyrophosphate, was also added to a final 1 U/mL. The reaction was quenched by boiling at 100 °C for 10min followed by concentration at 13,000 rpm for 30 min. Bio-gel P2 gel filtration column (Bio-Rad) was used to separate the product from the reaction mixture and the fractions containing CDP-GlcNAc product were pooled and lyophilized.

Acknowledgements

The authors acknowledge the support of National Basic Research Program of China (973 Program, No. 2012CB822102), the Key Grant Project of Chinese Ministry of Education (No. 313033), and Promotive Research Fund for Excellent Young and Middle-Aged Scientists of Shandong Province (No. BS2013SW023).

Supplementary data

Supplementary data related to this article can be found at http://dx.doi.org/10.1016/j.carres.2015.05.007.

References

1. Barbosa MD, Yang G, Fang J, Kurilla MG, Pompliano DL. *Antimicrob Agents Chemother* 2002;**46**:943–6.
2. Whitfield C, Trent MS. *Annu Rev Biochem* 2014;**83**:99–128.
3. Masuko S, Bera S, Green DE, Weiwer M, Liu J, DeAngelis PL, et al. *J Org Chem* 2012;**77**:1449–56.
4. Ovchinnikova OG, Rozalski A, Liu B, Knirel YA. *Biochemistry* 2013;**78**:798–817.
5. Zhang D, Wang PG, Qi Q. *Biotechnol Lett* 2007;**29**:1729–33.
6. Niemann MC, Bartrina I, Ashikov A, Weber H, Novak O, Spichal L, et al. *Proc Natl Acad Sci U.S.A* 2015;**112**:291–6.
7. Mohorko E, Glockshuber R, Aebi M. *J Inherit Metab Dis* 2011;**34**:869–78.
8. Chang R, Vo TT, Finney NS. *Carbohydr Res* 2006;**341**:1998–2004.
9. Zeng Y, Shabalin Y, Szumilo T, Pastuszak I, Drake RR, Elbein AD. *Anal Biochem* 1996;**239**:99–106.
10. Mengin-Lecreulx D, van Heijenoort J. *J Bacteriol* 1993;**175**:6150–7.
11. Mochalkin I, Lightle S, Zhu Y, Ohren JF, Spessard C, Chirgadze NY, et al. *Protein Sci* 2007;**16**:2657–66.
12. Kostrewa D, D'Arcy A, Takacs B, Kamber M. *J Mol Biol* 2001;**305**:279–89.
13. Han S, Forman MD, Loulakis P, Rosner MH, Xie Z, Wang H, et al. *J Mol Biol* 2006;**360**:814–25.
14. Brown K, Pompeo F, Dixon S, Mengin-Lecreulx D, Cambillau C, Bourne Y. *EMBO J* 1999;**18**:4096–107.
15. Olsen LR, Roderick SL. *Biochemistry* 2001;**40**:1913–21.
16. Fang J, Guan W, Cai L, Gu G, Liu X, Wang PG. *Bioorg Med Chem Lett* 2009;**19**:6429–32.
17. Nishimoto M, Kitaoka M. *Appl Environ Microbiol* 2007;**73**:6444–9.
18. Fang J, Xue M, Gu G, Liu XW, Wang PG. *Bioorg Med Chem Lett* 2013;**23**:4303–7.